

AD-A050 892

PENNSYLVANIA STATE UNIV UNIVERSITY PARK APPLIED RESE--ETC F/G 20/1
ON THE DIFFRACTION OF PLANE ACOUSTIC WAVES BY AN ELLIPSOIDALLY --ETC(U)
NOV 77 F H FENLON N00017-73-C-1418

UNCLASSIFIED

TM-77-314

NL

| OF |
AD
A050 892



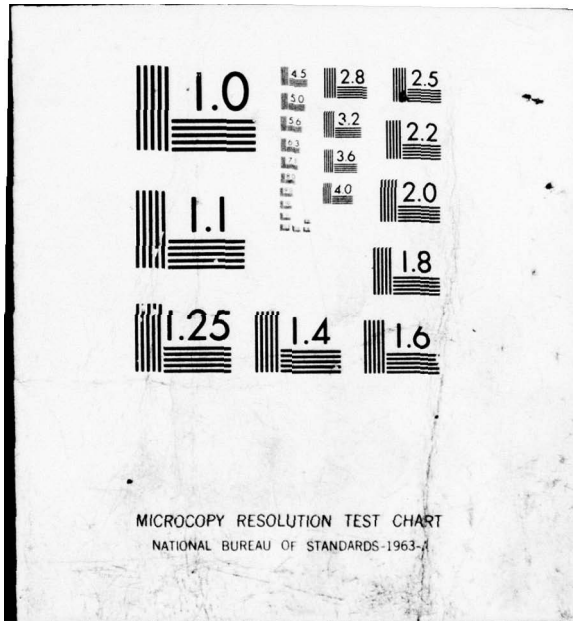
END

DATE

FILMED

4-78

DDC



UNCLASSIFIED

Handwritten mark

12

AD A 050892

ON THE DIFFRACTION OF PLANE ACOUSTIC WAVES BY AN
ELLIPSOIDALLY CAPPED ELASTIC CYLINDER OF ARBITRARY
IMPEDANCE

F. H. Fenlon

AD NO. _____
DDC FILE COPY

Technical Memorandum
File No. TM 77-314
November 17, 1977
Contract No. N00017-73-C-1418

Copy No. 9

DDC
MAR 8 1978
F

The Pennsylvania State University
Institute for Science and Engineering
APPLIED RESEARCH LABORATORY
P. O. Box 30
State College, PA 16801

NAVY DEPARTMENT
NAVAL SEA SYSTEMS COMMAND

DISTRIBUTION STATEMENT A
Approved for public release;
Distribution Unlimited

UNCLASSIFIED

UNCLASSIFIED

SECURITY CLASSIFICATION OF THIS PAGE (When Data Entered)

| REPORT DOCUMENTATION PAGE | | READ INSTRUCTIONS BEFORE COMPLETING FORM |
|--|-----------------------|--|
| 1. REPORT NUMBER <u>14</u> TM-77-314 | 2. GOVT ACCESSION NO. | 3. RECIPIENT'S CATALOG NUMBER |
| 4. TITLE (and Subtitle) <u>6</u> ON THE DIFFRACTION OF PLANE ACOUSTIC WAVES BY AN ELLIPSOIDALLY CAPPED ELASTIC CYLINDER OF ARBITRARY IMPEDANCE. | | 5. TYPE OF REPORT & PERIOD COVERED <u>9</u> Final report |
| | | 6. PERFORMING ORG. REPORT NUMBER |
| 7. AUTHOR(s) <u>10</u> F. H. Fenlon | | 8. CONTRACT OR GRANT NUMBER(s) <u>15</u> N00017-73-C-1418 |
| 9. PERFORMING ORGANIZATION NAME AND ADDRESS Applied Research Laboratory P. O. Box 30 State College, PA 16801 | | 10. PROGRAM ELEMENT, PROJECT, TASK AREA & WORK UNIT NUMBERS <u>11</u> |
| 11. CONTROLLING OFFICE NAME AND ADDRESS Naval Sea Systems Command Washington, DC 20362 | | 12. REPORT DATE <u>17 Nov 77</u> November 17, 1977 |
| | | 13. NUMBER OF PAGES <u>42</u> 39 p. |
| 14. MONITORING AGENCY NAME & ADDRESS (if different from Controlling Office) | | 15. SECURITY CLASS. (of this report) Unclassified |
| | | 15a. DECLASSIFICATION/DOWNGRADING SCHEDULE |
| 16. DISTRIBUTION STATEMENT (of this Report) Approved for public release; distribution unlimited; per NAVSEA Dec. 22, 1977. | | |
| 17. DISTRIBUTION STATEMENT (of the abstract entered in Block 20, if different from Report) | | |
| 18. SUPPLEMENTARY NOTES | | |
| 19. KEY WORDS (Continue on reverse side if necessary and identify by block number) diffraction transducer array plane waves cylinder | | |
| 20. ABSTRACT (Continue on reverse side if necessary and identify by block number) In this paper, the Geometrical Theory of Diffraction is used to investigate the effect of diffraction on the back response of transducer array elements mounted on the flat face of an ellipsoidally capped cylinder of arbitrary acoustic impedance. | | |

DDC
MAR 8 1978
F

391 φφ7

UNCLASSIFIED

Subject: On the Diffraction of Plane Acoustic Waves
by an Ellipsoidally Capped Elastic Cylinder
of Arbitrary Impedance (U)

ABSTRACT

(U) In this paper the Geometrical Theory of Diffraction is used to investigate the effect of diffraction on the back response of transducer array elements mounted on the flat face of an ellipsoidally capped cylinder of arbitrary acoustic impedance.

| | |
|---------------------------------|---|
| ACCESSION FOR | |
| NTIS | W. E. Section <input checked="" type="checkbox"/> |
| DDC | B. M. Section <input type="checkbox"/> |
| UNANNOUNCED | |
| J. S. I. CATION | |
| BY | |
| DISTRIBUTION/AVAILABILITY CODES | |
| IN | SPECIAL |
| A | |

UNCLASSIFIED

TABLE OF CONTENTS

| | <u>Page</u> |
|-----------------------------|-------------|
| ABSTRACT | 1 |
| TABLE OF CONTENTS | 2 |
| LIST OF FIGURES | 3 |
| LIST OF TABLES | 4 |
| LIST OF SYMBOLS | 5 |
| ACKNOWLEDGMENT | 7 |
| Introduction | 8 |
| Theory | 12 |
| Conclusions | 24 |
| APPENDIX A | 28 |
| APPENDIX B | 34 |
| APPENDIX C | 36 |
| REFERENCES | 37 |

LIST OF FIGURES

| <u>Figure</u> | <u>Page</u> |
|---|-------------|
| 1a. Directional Response of a Transducer Array Element - Source in the Insonified Zone of the Array | 9 |
| 1b. Directional Response of a Transducer Array Element - Source in the Shadow Zone of the Array | 9 |
| 2a. GTD Parameters of a Diffracted Wave Field on an Arbitrary Surface of Revolution | 16 |
| 2b. GTD Parameters of a Diffracted Wave Field on an Ellipsoidally Capped Cylinder | 17 |
| 3a. Directivity Pattern of a Centrally Located Receiver Element in a Plane Array Mounted at the Head of an Ellipsoidally Capped Cylinder of Uniform Surface Impedance, $Z_p = Z_a = 20$ | 25 |
| 3b. Directivity Pattern of a Centrally Located Receiver Element in a Plane Array Mounted at the Head of an Ellipsoidally Capped Cylinder of Uniform Surface Impedance, $Z_p = Z_a = 2$ | 25 |
| 4a. Directivity Pattern of a Centrally Located Receiver Element in a Plane Array Mounted at the Head of an Ellipsoidally Capped Cylinder of Nonuniform Surface Impedance, $Z_p = 20, Z_a = 10$ | 26 |
| 4b. Directivity Pattern of a Centrally Located Receiver Element in a Plane Array Mounted at the Head of an Ellipsoidally Capped Cylinder of Nonuniform Surface Impedance, $Z_p = 20, Z_a = 2$ | 26 |
| 4c. Directivity Pattern of a Centrally Located Receiver Element in a Plane Array Mounted at the Head of an Ellipsoidally Capped Cylinder of Nonuniform Surface Impedance, $Z_p = 20, Z_a = 0.1$ | 26 |

LIST OF TABLES

| <u>Table</u> | <u>Page</u> |
|--|-------------|
| 1a. Comparison of Levy Keller's ⁵ and Pathak Kouyoumjian's ⁶ Diffraction and Attenuation Coefficients for Variable Radius-of-Curvature, Impedance Surfaces | 18 |
| 1b. Numerical Comparison of Parameters Implicit in the Two Notational Forms of Table 1a. | 19 |

LIST OF SYMBOLS

| | |
|--|---|
| p, p_i, p_r, p_d | Total pressure field, incident, reflected, and diffracted pressure fields, respectively |
| \underline{v} | Particle velocity |
| θ, θ_o | Angle of incidence, and receiver element coordinate, respectively |
| $\psi = \theta - \frac{\pi}{2}$ | Intermediate angle |
| $\frac{\partial}{\partial \eta}$ | Gradient in the direction of the outward normal to a surface |
| $R(\theta)$ | Reflection coefficient |
| $D(\theta)$ | Directivity pattern |
| ρ_o, ρ_p | Density of the fluid medium, and of a flat plate, respectively |
| c_o, c_p | Speed of sound in the fluid medium, and in a flat plate, respectively |
| $\rho c, \rho_p c_p$ | Characteristic impedance of the fluid medium and of plate material, respectively |
| ϕ_e, ϕ_a | Scalar electromagnetic and acoustic potential, respectively |
| z_p | Plate impedance |
| $Z_p = z_p / \rho c$ | Plate impedance normalized with respect to the characteristic impedance of the fluid |
| Z_e, Z_a | Normalized electromagnetic and acoustic curved surface impedance, respectively |
| E_p, σ_p | Young's modulus and Poisson's ratio for a flat plate |
| h | Plate thickness |
| $\Omega = \omega / \omega_o$ | Ratio of angular frequency ω to plate coincidence frequency ω_o |
| $\omega_o = \frac{\sqrt{12}}{h} \frac{c_o^2}{c_p}$ | Angular coincidence frequency of a flat plate of thickness h |
| $k = \omega / c_o$ | Wavenumber in the fluid |
| $\rho_*, \rho_*^o = b^2 / a$ | Radius-of-curvature, and minimum radius-of-curvature of an ellipse of revolution |

| | |
|------------------------------------|---|
| r_b | Radius of a cylindrical body |
| b, a | Semi-minor and semi-major axes of an ellipse |
| $\kappa = \sqrt{1 - (b/a)^2}$ | Eccentricity |
| $h_b = r_b - b$ | Radius of the flat front of an ellipsoidally capped cylinder |
| R | Distance from the source to the point of incidence |
| S | Distance from the point of departure on the body to the receiver |
| t | Distance over a curved surface between the points of incidence and departure, respectively |
| a_0, a_1, ρ_1 | Geometrical parameters |
| α_n^{LK}, α_n | Attenuation Coefficients for diffracted waves defined by Levy and Keller ² and Pathak and Kouyoumjian, ⁴ respectively |
| D_n^{LK}, D_n | Diffraction coefficients defined by Levy and Keller ² and Pathak and Kouyoumjian, ⁴ respectively |
| $A_{LK}, A'_{LK}; A_i, A'_i$ | Airy functions and their derivatives in Levy and Keller's ² and Pathak and Kouyoumjian's, ⁴ respective notations |
| $q_n^{LK}, q_n = q_n^{LK}/3^{1/3}$ | Roots of the impedance equation in Levy and Keller's ² and Pathak and Kouyoumjian's ⁴ notations, respectively |
| $\tau_n = q_n^{LK}/6^{1/3}$ | Roots of the 'Tangent Equation' |
| $J_n, H_n^{(1)}, H_n^{(2)}$ | Bessel and Hankel functions, respectively |

ACKNOWLEDGMENT

The author is particularly indebted to Mr. F. S. McKendree for his skillful programming of the analytical model discussed herein.

Introduction

This paper is concerned with the problem of analytically modeling the acoustic fields that control the directional response of transducer array elements mounted on the flat face of an ellipsoidally capped cylinder, such as that depicted schematically in Figure 1. The basic objective is to investigate the extent to which the back-to-front ratios of individual transducer array element directivity patterns can be minimized by reducing the diffracted fields which reach them from the rear of the body via propagation over the curved surface.

The measurement procedure to be modeled is plane wave insonification of the array elements with the source in the far-field of the body, as depicted schematically in Figures 1a and 1b; the former with the source in the 'insonified zone of the array' (i.e., $0 \leq \theta \leq \pi/2$), depicting the combined incident, reflected, and diffracted fields normalized with respect to the incident field; the latter, with the source in the 'shadow zone of the array' (i.e., $\pi/2 < \theta \leq \pi$), depicting the field diffracted around the curved surface of the body to the array element, again normalized with respect to the incident field. Note that when the terms 'insonified zone' or 'shadow zone' of the array are used here, the field at the source is regarded by reciprocity to be produced via radiation from the array.

In order to describe the diffracted field analytically, we make use of Keller's^{1,2} Geometrical Theory of Diffraction (GTD). This method effectively permits ray tracing over curved impedance surfaces where the only part of a ray tube that can propagate are tangent rays (i.e., Franz³ waves, analogous to Stoneley waves which occur at almost grazing incidence on insonified flat elastic surfaces immersed in liquids). Since the diffracted field sheds rays at each point of tangency as it propagates along a curved surface, the

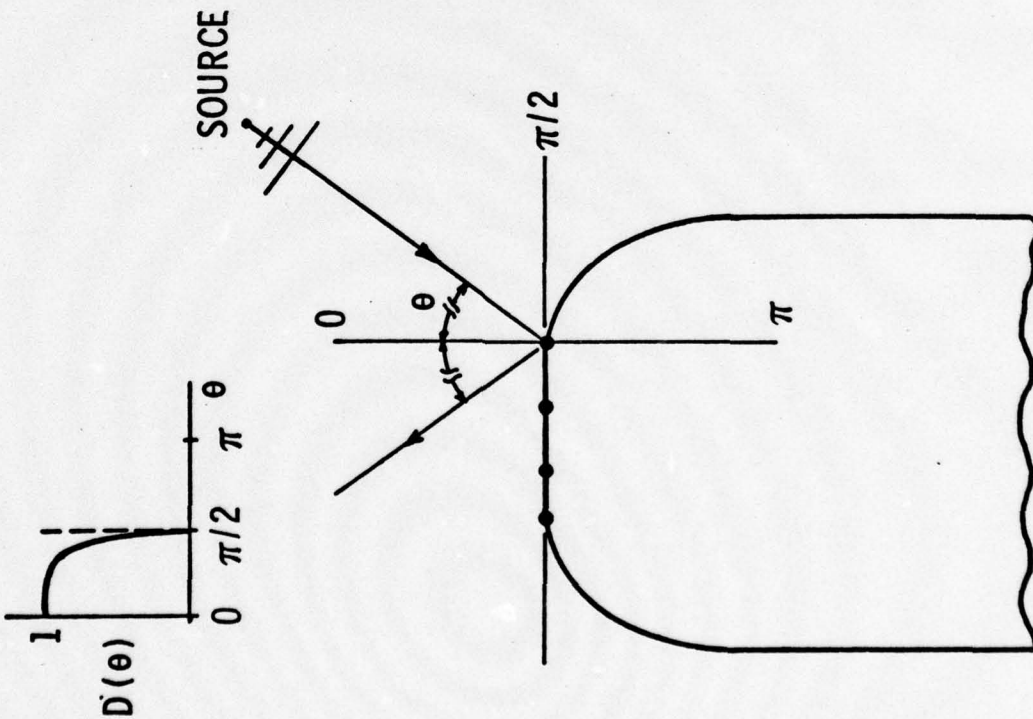


Figure 1a. Directional Response of a Transducer Array Element - Source in the Insonified Zone of the Array

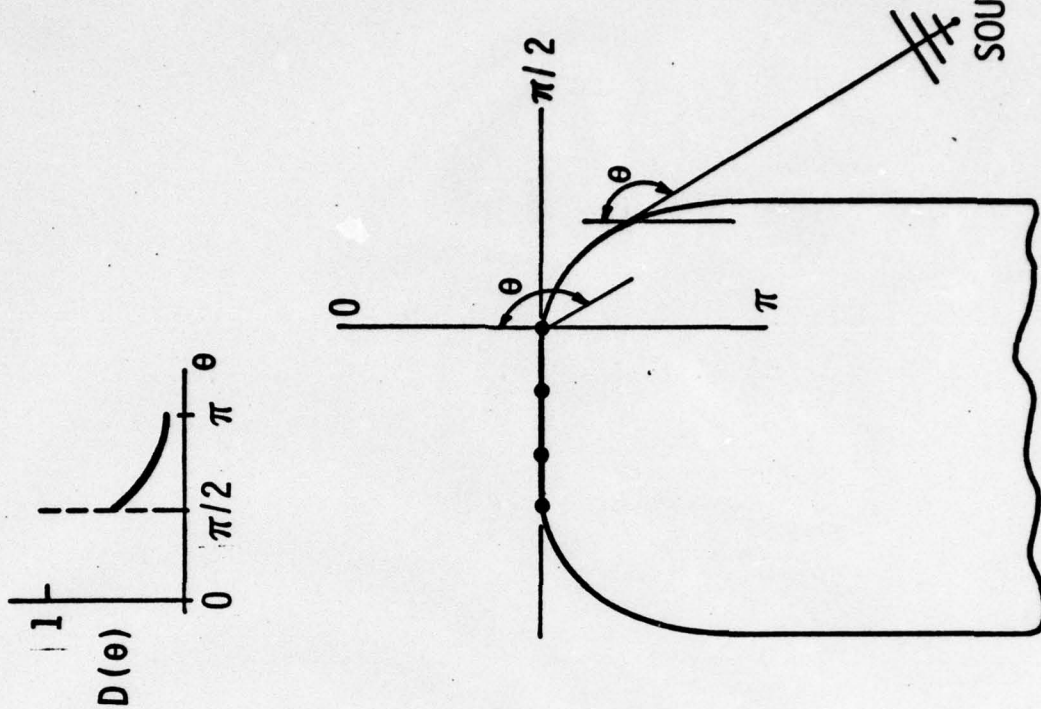


Figure 1b. Directional Response of a Transducer Array Element - Source in the Shadow Zone of the Array

energy flux diminishes in a manner phenomenologically attributable to an exponential field decay with geodesic distance from the point of insonification. Now the 'attenuation coefficient' of this decay is dependent on the local radius-of-curvature of the body and on the local surface impedance, the latter dependence being a consequence of the manner in which the impedance affects re-radiation of the diffracted field at each point of the surface. Thus, for example, the diffracted field on an acoustically rigid curved surface is re-radiated at each point of the surface by a monopole source distribution. This, in turn, is more efficient than the dipole source distribution associated with an acoustically soft (i.e., pressure release) surface. Consequently, the 'attenuation' per wavelength of surface rays propagating on an acoustically soft curved surface is considerably greater than that on an acoustically hard curved surface. Since materials which are 'rigid' in air appear acoustically more compliant in water, we note at this point that 'rigid' in water implies an impedance of at least an order-of-magnitude greater than the characteristic impedance of the fluid.

The 'diffraction' and 'attenuation' coefficients of Keller's¹ Theory are obtained from 'canonical problems' i.e., those that are amenable to exact solution, such as creeping wave solutions for separable coordinate surfaces of the Helmholtz equation, in particular surfaces of constant curvature (e.g. infinite cylinders and spheres). For these basic or canonical surfaces the creeping wave solutions are obtained by re-expressing the exact eigenfunction solutions (whose rate of convergence deteriorates with increasing values of $k\rho_*$) in the form of Luneberg-Kline series whose terms decrease as $(1/k\rho_*)^n$, $n = 1, 2, \dots$. Whenever $k\rho_* \gg 1$, it follows that only the first few terms of these reconditioned series are required to provide an accurate representation of the diffracted field. In the case

of a surface of variable radius-of-curvature the first few terms of these canonical series can also be used to describe the diffracted field over local regions of the surface where the radius-of-curvature is slowly varying, although a note of caution should be added in the light of Leppington's⁴ analysis. Generally speaking, however, 'diffraction' and 'attenuation' coefficients for a variable radius-of-curvature surface can be expressed in terms of its impedance and differential geometry as shown by Levy and Keller.⁵

Before concluding these remarks a point of confusion between electromagnetic and acoustic analogues should be mentioned. This point concerns the application of the electromagnetic impedance boundary conditions to acoustic problems, i.e. as given by Keller¹

$$\frac{\partial \phi_e}{\partial \eta} = ikZ_e \phi_e, \quad (1a)$$

where ϕ_e is the scalar e.m. potential, and Z_e is the e.m. surface impedance relative to the characteristic impedance of the surrounding medium. In an acoustic field, however, since the particle velocity is given by definition as $\underline{v} = \nabla \phi_a$ and for sinusoidal disturbances the pressure is given by $p = -i\rho_0 c_0 k \phi_a$, the impedance relationship $p = z_a |v|$ at the surface of a body becomes,

$$\frac{\partial \phi_a}{\partial \eta} = -ikZ_a^{-1} \phi_a, \quad (1b)$$

where ϕ_a is the acoustic field potential, and $Z_a = z_a / \rho c$ is the acoustic surface impedance relative to the characteristic impedance of the fluid medium. From inspection of Equations (1a) and (1b) it follows

that whenever the acoustic analogue of a corresponding e.m. diffraction problem is invoked, Z_e should be replaced by Z_a^{-1} yielding the relationships between diffraction and attenuation coefficients summarized by Pathak and Kouyoumjian.⁶

Theory

We begin by considering the axisymmetric insonification of an ellipsoidally capped cylinder such as that depicted schematically in Figures 1a and 1b by a point source in the far-field of the body. For the case of a circular piston of diameter d mounted on the flat front-end surface, the received field can be expressed as,

$$P = P_i + P_r + P_d, \quad (2)$$

where P_i, P_r , and P_d denote the incident, reflected, and diffracted fields, respectively. When the source is located in the first quadrant (i.e., in the insonified zone of the array, $0 \leq \theta \leq \frac{\pi}{2}$), if the length of the body is sufficient to ensure the effective attenuation of diffracted waves before they arrive at the receiver elements via propagation around the body, the field received by an element from 0° to 90° will only depend upon the incident and reflected waves. In this instance therefore,

$$P = P_i + P_r, \quad P_d = 0, \quad 0 \leq \theta \leq \frac{\pi}{2}. \quad (3a)$$

On the other hand, when the source is in the second quadrant (i.e., $\frac{\pi}{2} < \theta \leq \pi$), only diffracted waves reach the array elements, so that in the shadow zone of the array,

$$p = p_d , \quad \frac{\pi}{2} < \theta \leq \pi . \quad (3b)$$

In the third quadrant the field is again given by Equation (3b) and in the fourth quadrant by Equation (3a).

Between the insonified zone and the deep shadow zone of the array there is a region described as the transition zone which approximately spans the sector $\pi/2 - (k\rho_*^0/2)^{-1/3} \leq \theta \leq \pi/2 + (k\rho_*^0/2)^{-1/3}$. In this region, the field is governed by incident, reflected, and diffracted waves. One consequence of the transition zone is that the directivity pattern or directional response of a receiver element normalized with respect to its response on boresight, is reduced by 50% at $\theta = \pi/2$ on uniformly hard (i.e., $Z_a = \infty$) and soft baffles (i.e., $Z_a = 0$). Under these conditions, as Pathak and Kouyoumjian⁶ have shown for analogous e.m. problems, the transition zone field can be described analytically by means of Fock functions. However, the derivation of a suitable transition zone approximation for an arbitrary impedance baffle has yet to be resolved, and consequently the exact value of a receiver element's response at $\theta = \pi/2$ remains unspecifiable. For this reason, in our subsequent numerical analysis, we compute the response from 0 to $\pi/2 - (k\rho_*^0/2)^{-1/3}$ and from $\pi/2 + (k\rho_*^0/2)^{-1/3}$ to π , joining the two regions graphically via matching slopes. Although this procedure cannot be rigorously justified, it does not in any way detract from our computation of the response in the deep shadow zone, which is the primary task of this investigation.

Concentrating on the field in the insonified zone, Equation (3a) can be re-expressed in the form,

$$p = p_1 \{1 + R(\theta)\} , \quad 0 \leq \theta \leq \frac{\pi}{2} . \quad (4)$$

where the reflection coefficient $R(\theta)$ is defined as,

$$R(\theta) = \frac{Z_p(\theta) \cos(\theta - \theta_o) - 1}{Z_p(\theta) \cos(\theta - \theta_o) + 1}, \quad (5)$$

$Z_p(\theta)$ being the angle-dependent plate impedance of the flat face, normalized with respect to the characteristic impedance ρc of the medium in which the body is located, i.e., as summarized by Hayek and Stuart,⁷

$$Z_p(\theta) = -i(k_p h)(\rho_p c_p / \rho c) \{ \Omega^2 \sin^4(\theta - \theta_o) - 1 \}, \quad k_p = \omega / c_p. \quad (6)$$

In this notation, ρ_p is the mass density of the plate and c_p is the phase velocity of plate waves which in turn is a function of the Young's modulus E_p and Poisson's ratio σ_p of the plate given by

$$c_p^2 = \frac{E_p}{(1 - \sigma_p^2) \rho_p}. \quad (7)$$

Again $\Omega = \omega / \omega_o$ (8)

where $\omega_o = \frac{\sqrt{12}}{h} \frac{c_p^2}{c_p}$ is the coincidence frequency for a plate of thickness h . (9)

Substituting Equation (5) in Equation (4) and multiplying by the directional response function of a circular piston of diameter d , the resulting directivity pattern of a receiver located at the point (r_o, θ_o) on the flat face of the body can be expressed as,

$$D(\theta) = p/p_1$$

$$= \left\{ \frac{2Z_p(\theta) \cos(\theta - \theta_o)}{1 + Z_p(\theta) \cos(\theta - \theta_o)} \right\} \left\{ \frac{2J_1\left[\frac{kd}{2} \sin(\theta - \theta_o)\right]}{\frac{kd}{2} \sin(\theta - \theta_o)} \right\} e^{ikr_o \cos(\theta - \theta_o)},$$

$$0 \leq \theta - \theta_o \leq \frac{\pi}{2} \quad (10)$$

We now consider the back response of a receiver element due to diffracted waves which occur when the source is located in the shadow zone of the array, $\pi/2 < \theta \leq \pi$. From Levy and Keller's⁵ fundamental analysis, this field can be represented via the Geometrical Theory of Diffraction as,

$$p_d = \frac{e^{ikR}}{4\pi R} \left\{ \frac{a_o \rho_1}{sa_1(\rho_1 + s)} \right\}^{1/2} \sum_{n=0}^N D_n^{LK}(P_1) D_n^{LK}(P_2) e^{ik(t+S)} - \int_{P_1}^{P_2} \alpha_n^{LK}(t') dt' \quad (11)$$

The parameters a_o , a_1 , ρ_1 , S , t , and R which appear in this equation are shown in Figure 2a for diffracted waves traveling over an arbitrary curved surface from the point of insonification P_1 to the point of departure P_2 . Analytical expressions for the diffraction and attenuation coefficients D_n^{LK} and α_n^{LK} , respectively, deduced by Levy and Keller⁵ are compared in Table 1a with similar expressions resulting from a different definition of the Airy Function as summarized by Pathak and Kouyoumjian⁶ - numerical comparisons being presented in Table 1b. A brief synopsis of the steps inherent in the derivation of these coefficients is also included for the benefit of the reader in Appendix A.

For the case of the axisymmetric ellipsoidally capped cylinder depicted in Figure 2b, the variable radius-of-curvature ρ_* of the elliptical section is given by,

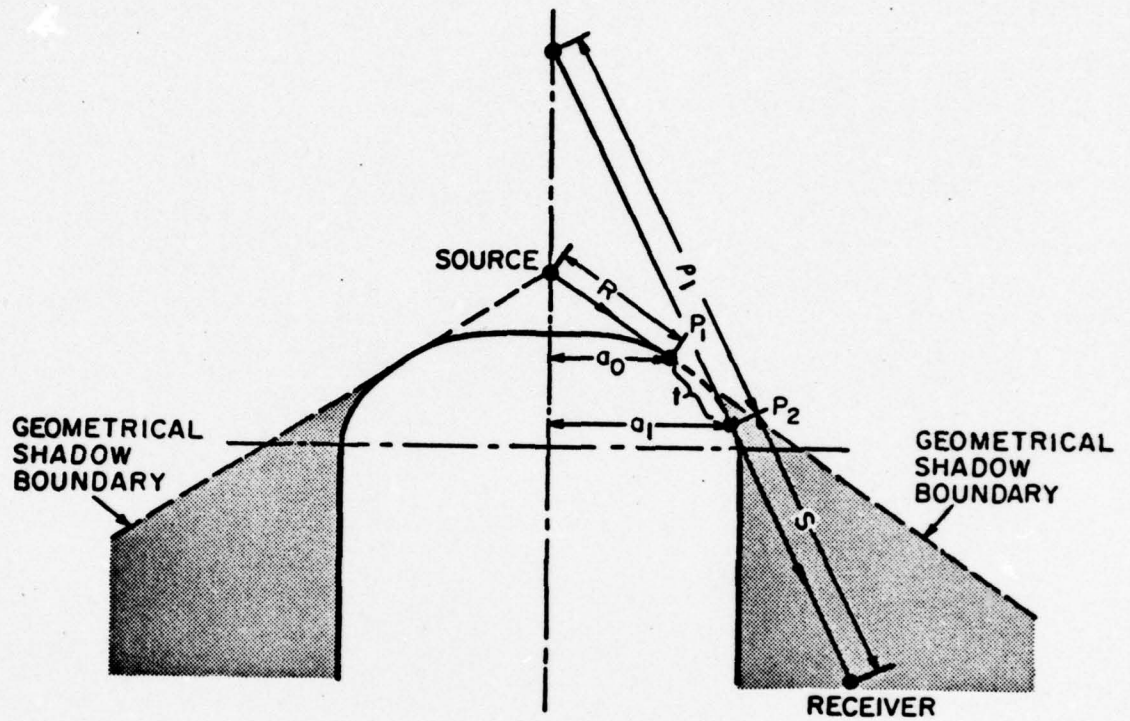


Fig. 2a GTD Parameters of a Diffracted Wave Field on an Arbitrary Surface of Revolution

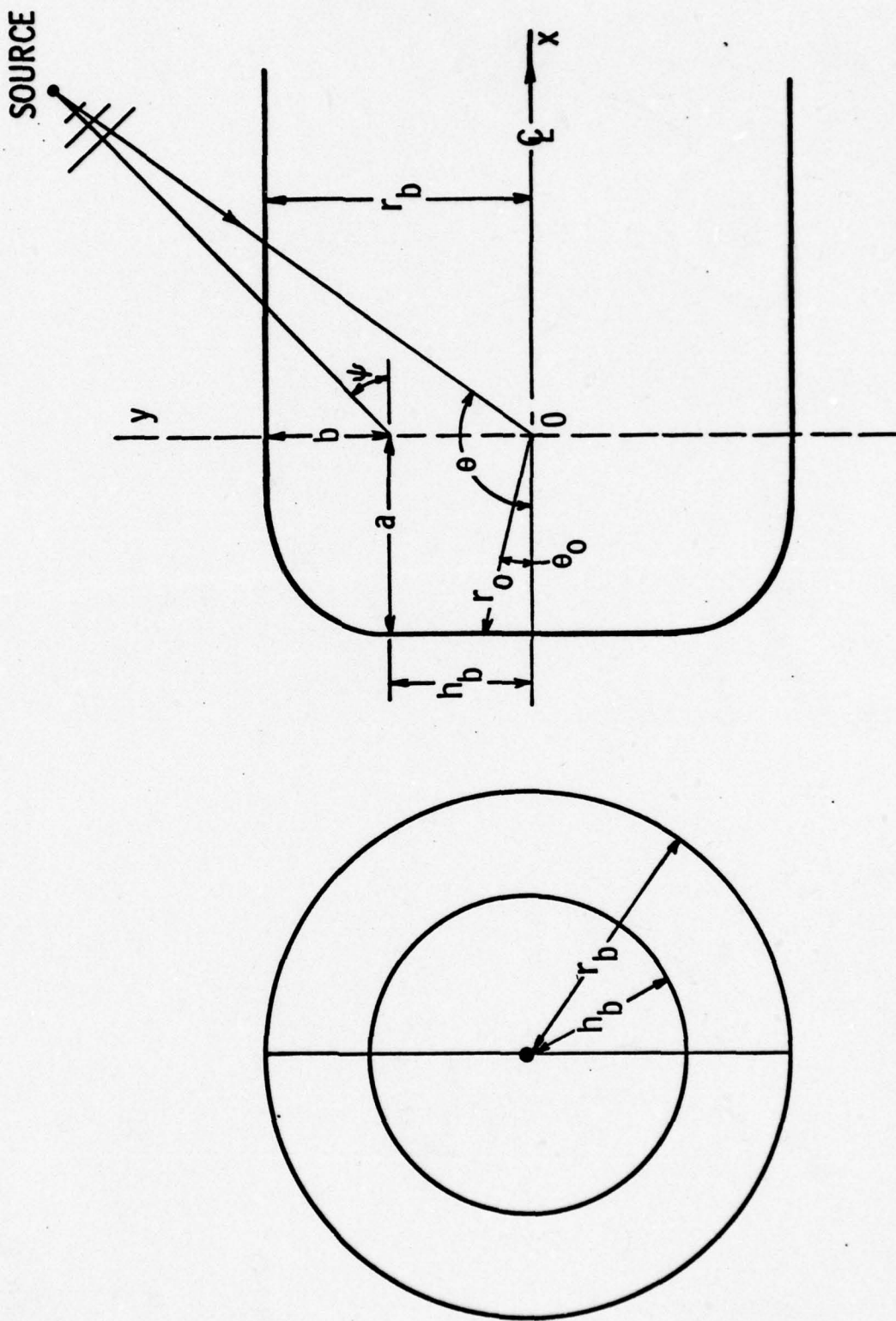


Fig. 2b GTD Parameters of a Diffracted Wave Field on an Ellipsoidally Capped Cylinder

| | Levy and Keller ⁵ | Pathak and Kouyoumjian ⁶ |
|-----------------------------------|---|--|
| Airy Function | $A_{LK}(-X_{LK}) = \int_0^\infty \cos(t^3 - X_{LK} t) dt$ | $A_1(-X) = \frac{1}{\pi} \int_0^\infty \cos(t^3/3 - X t) dt$ |
| Square of Diffraction Coefficient | $(D_n^{LK})^2 = \frac{\pi^{3/2} 2^{-1/2} 6^{-1/3} k^{-1/6} \rho_g^{1/3} e^{-i\pi/12}}{3A_{LK}^2(-q_n^{LK}) + q_n^{LK} A_{LK}^2(-q_n^{LK})}$ | $D_n^2 = \frac{\pi^{-1/2} 2^{-5/6} k^{-1/6} \rho_g^{1/3} e^{-i\pi/12}}{A_1^2(-q_n) + q_n A_1^2(-q_n)}$ |
| Attenuation Coefficient | $\alpha_n^{LK} = (q_n^{LK}/\rho_{*}) (k\rho_{*}/6)^{1/3} e^{i\pi/6}$ | $\alpha_n = (q_n/\rho_{*}) (k\rho_{*}/2)^{1/3} e^{i\pi/6}$ |
| Impedance Relationship | $\frac{A_{LK}'(-q_n^{LK})}{A_{LK}(-q_n^{LK})} = e^{-15\pi/6} (k\rho_{*}/6)^{1/3} Z_a^{-1}$ | $\frac{A_1'(-q_n)}{A_1(-q_n)} = e^{-15\pi/6} (k\rho_{*}/2)^{1/3} Z_a^{-1}$ |
| Roots | q_n^{LK} | $q_n = q_n^{LK}/3^{1/3}$ |

Table 1a.

Comparison of Levy Keller's⁵ and Pathak Kouyoumjian's⁶ Diffraction and Attenuation Coefficients for Variable Radius-of-Curvature, Impedance Surfaces

$$q_n^{LK} = 6^{1/3} \tau_n e^{i\pi/3} \text{ from Equation (B2)} ; \quad A_{LK}(-q_n^{LK}) = \frac{\pi}{3^{1/3}} A_1(-q_n) , \text{ from Equation (A18)}$$

$$= 3^{1/3} q_n , \text{ from Equation (A20)} ; \quad A'_{LK}(-q_n^{LK}) = -\frac{\pi}{3^{2/3}} A'_1(-q_n) , \text{ from Equation (A19)}$$

| Parameters | Hard Acoustic Surface, $Z_a = \infty$ | Soft Acoustic Surface, $Z_a = 0$ |
|----------------------|---------------------------------------|----------------------------------|
| τ_0 | $0.8086166 e^{-i\pi/3}$ | $1.8557571 e^{i\pi/3}$ |
| τ_1 | $2.5780962 e^{-i\pi/3}$ | $3.2446076 e^{i\pi/3}$ |
| q_0^{LK} | 1.46935 | 3.37213 |
| q_1^{LK} | 4.68417 | 5.89584 |
| q_0 | 1.01879 | 2.33811 |
| q_1 | 3.24820 | 4.08795 |
| $A_{LK}(-q_0^{LK})$ | 1.16680 | 0.0 |
| $A_{LK}(-q_1^{LK})$ | -0.91273 | 0.0 |
| $A'_{LK}(-q_0^{LK})$ | 0.0 | -1.05905 |
| $A'_{LK}(-q_1^{LK})$ | 0.0 | 1.21295 |
| $A_1(-q_0)$ | 0.53566 | 0.0 |
| $A_1(-q_1)$ | -0.41902 | 0.0 |
| $A'_1(-q_0)$ | 0.0 | 0.70121 |
| $A'_1(-q_1)$ | 0.0 | -0.80311 |

Table 1b.

Numerical Comparison of Parameters Implicit in the Two Notational Forms of Table 1a

$$\begin{aligned}\rho_* &= - \frac{(1 + y'^2)^{3/2}}{y''} \\ &= \frac{b^2}{a} \left\{ 1 + \left(\frac{a^2 - b^2}{b^4} \right) (y - h_b)^2 \right\}^{3/2} .\end{aligned}\quad (12)$$

Following Sachs,⁸ who considered the case of a source located on the cylindrical surface of the body rather than as herein envisaged in the far field, we let

$$x = a \sin \psi , \quad y = h_b + b \cos \psi . \quad (13)$$

Equation (12) thus becomes,

$$\rho_* = \frac{a^2}{b} \left\{ 1 - \kappa^2 \sin^2 \psi \right\}^{3/2} , \quad \kappa^2 = 1 - \frac{b^2}{a^2} . \quad (14)$$

Likewise, for far-field insonification of the body, the distance t on the ellipsoidally curved surface between an arbitrary point of incidence P_1 and the exit point P_2 of the diffracted field at the flat face is given by,

$$t = a \int_0^\psi \{ 1 - \kappa^2 \sin^2 \psi \}^{1/2} d\psi . \quad (15)$$

From Table 1 and Equation (15), the integral of the attenuation coefficients α_n^{LK} in Equation (11) over the interval t from P_1 to P_2 of the ellipsoidal surface can be expressed as,

$$\begin{aligned}
 \int_{P_1}^{P_2} \alpha_n^{\text{LK}}(t') dt' &= \int_0^t \alpha_n^{\text{LK}}(t') dt' \\
 &= \int_0^\psi \alpha_n^{\text{LK}}(\psi) \frac{dt'}{d\psi} d\psi \\
 &= e^{i\pi/6} (kb^2/6a)^{1/3} \int_0^\psi \frac{q_n^{\text{LK}}(\psi) d\psi}{\sqrt{1 - \kappa^2 \sin^2 \psi}} \quad (16)
 \end{aligned}$$

where q_n^{LK} are the roots of the transcendental equation

$$\frac{A'_{\text{LK}}[-q_n^{\text{LK}}(\psi)]}{A_{\text{LK}}[-q_n^{\text{LK}}(\psi)]} = (ka^2/6b)^{1/3} e^{i5\pi/6} (1 - \kappa^2 \sin^2 \psi)^{1/2} z_a^{-1}(\psi), \quad (17)$$

this equation being deduced in Appendix A from the boundary conditions for a finite impedance surface. In practice, however, for a finite impedance surface it is preferable to compute the roots via the alternative 'tangent equation' derived by Keller,¹ as outlined in Appendix B.

Now the diffraction coefficients at the point of incidence $D_n^{\text{LK}}(P_1)$ are given by,

$$D_n^{\text{LK}}(P_1) = \sqrt{\frac{\pi^{3/2} 2^{-1/2} 6^{-1/3} (ab/k)^{1/6} e^{-i\pi/12} (1 - \kappa^2 \sin^2 \psi)^{1/2}}{3A_{\text{LK}}^2(q_n^{\text{LK}}) + q_n^{\text{LK}} A_{\text{LK}}^2(q_n^{\text{LK}})}}, \quad (18)$$

whilst those at the exit point, $D_n^{\text{LK}}(P_2)$ are given by,

$$D_n^{\text{LK}}(P_2) = \sqrt{\frac{\pi^{3/2} 2^{-1/2} 6^{-1/3} (ab/k)^{1/6} e^{-i\pi/12}}{3A_{\text{LK}}^2(q_n^{\text{LK}}) + q_n^{\text{LK}} A_{\text{LK}}^2(q_n^{\text{LK}})}}. \quad (19)$$

If the curvature of the surface is uniform then,

$$D_n^{\text{LK}}(P_1) D_n^{\text{LK}}(P_2) = \frac{\pi^{3/2} 2^{-1/2} 6^{-1/3} (ab/k)^{1/6} (1 - \kappa^2 \sin^2 \psi)^{1/4} e^{-i\pi/12}}{3A_{\text{LK}}^2(q_n^{\text{LK}}) + q_n^{\text{LK}} A_{\text{LK}}^2(q_n^{\text{LK}})} \quad (20)$$

If as in the present instance, however, the surface curvature is nonuniform then,

$$D_n^{LK}(P_1) D_n^{LK}(P_2) = \frac{\pi^{3/2} 2^{-1/2} 6^{-1/3} (ab/k)^{1/6} (1 - \kappa^2 \sin^2 \psi)^{1/4} e^{-i\pi/12}}{\sqrt{[3A_{LK_1}'^2(q_n^{LK_1}) + q_n^{LK_1} A_{LK_1}^2(q_n^{LK_1})][3A_{LK_2}'^2(q_n^{LK_2}) + q_n^{LK_2} A_{LK_2}^2(q_n^{LK_2})]}} \quad (21)$$

where $q_n^{LK_1}$ and $q_n^{LK_2}$ are the roots of Equation (17) at the incident and exit points, respectively, of the curved surface in the shadow zone; A_{LK_1} , A_{LK_2}' ($i = 1, 2$) being the corresponding Airy functions and their derivatives evaluated at these roots, respectively.

Invoking reciprocity for an individual receiver element mounted on the flat face at the head of the capped cylinder insonified by a point source in the far-field, we have,

$$S = \infty, \quad a_o = h_b, \quad \rho_1/a_1 \approx |\cot \theta|, \quad \psi \approx \pi - \theta, \quad R = h_b(1 - \frac{r_o}{h_b} \sin \theta_o), \quad (22)$$

(r_o, θ_o) being the coordinates of the element relative to the axes through the center of the ellipsoid. Via reciprocity,

$$p_i = \lim_{S \rightarrow \infty} \frac{e^{ikS}}{S}, \quad \frac{\pi}{2} < \theta \leq \pi. \quad (23)$$

The directivity pattern of the receiver element due to insonification in the shadow zone, as defined by Equation (11), becomes

$$D(\theta) = p_d/p_i ;$$

$$= \left[\frac{|\cot \theta|^{1/2}}{(1 - \frac{r_o}{h_b} \sin \theta_o) h_b^{1/2}} \exp\{ikh_b(1 - \frac{r_o}{h_b} \sin \theta_o) + ika \int_0^{\theta - \frac{\pi}{2}} (1 - \kappa^2 \sin^2 \psi)^{1/2} d\psi\} \right]$$

$$\times \left[\sum_{n=0}^N D_n^{LK}(P_1) D_n^{LK}(P_2) \exp\{-e^{i\pi/6} (kb^2/6a)^{1/3} \int_0^{\theta - \frac{\pi}{2}} \frac{q_n(\psi) d\psi}{\sqrt{1 - \kappa^2 \sin^2 \psi}}\} \right] \quad (24)$$

UNCLASSIFIED

the product $D_n^{LK}(P_1) D_n^{LK}(P_2)$ being defined by Equations (20) and (21). It should be noted however, that when we are dealing with an edge element the terms in Equation (24) must be multiplied by the coefficients defined in Appendix C.

In order to test the analytical consistency of Equation (24) we now consider the case where the insonifying source is located on the cylindrical surface of the body at a distance x_0 from the origin of the coordinate system along the axis. This geometry requires that

$$S = x_0, \quad a_0 = h_b, \quad a_1 = r_b, \quad \rho_1 = \infty, \quad \theta = \pi, \quad R = h_b. \quad (25)$$

Hence, for a uniform impedance surface, substitution of Equations (25), (20), and (16) in Equation (11) with $2^{1/2} 6^{1/3} = 3^{1/3} 2^{5/6}$ gives,

$$P_d = \left[\frac{\pi^{1/2} (ab/k)^{1/6} e^{ik(h_b + x_0 + a)} \int_0^{\pi/2} (1 - \kappa^2 \sin^2 \psi)^{1/2} d\psi - i\pi/12}{4 \times 3^{1/3} \times 2^{5/6} \sqrt{h_b r_b x_0}} \right] \times \sum_{n=0}^N \frac{\exp[e^{i\pi/6} (kb^2/6a)^{1/3} q_n^{LK} \int_0^{\pi/2} \frac{d\psi}{\sqrt{1 - \kappa^2 \sin^2 \psi}}]}{q_n^{LK} A_{LK}^2(q_n^{LK})}. \quad (26)$$

If $|q_n^{LK}/6^{1/3}| \equiv |\tau_n| = \frac{1}{2}[3\pi(4n+3)/4]^{2/3}$, then Equation (26) is identical to that derived by Sachs.⁸ However, as shown in Appendix B, these roots are applicable when the baffle is acoustically soft. For the hard baffle condition therefore, the correct roots are given by Equation (B6), i.e., $|q_n^{LK}/6^{1/3}| \equiv |\tau_n| = \frac{1}{2}[3\pi(4n+1)/4]^{2/3}$, the erroneous choice of roots in Sachs'⁸ paper resulting, as mentioned in the Introduction, from a failure to distinguish the electromagnetic from the acoustic boundary conditions.

Returning to Equation (24) we now make use of Equations (10) and (21) to compute the diffraction pattern of a centrally located transducer array element, for a uniform impedance baffle with $Z_p = Z_a$ varying from 2 to 20 as $k\rho_*^0$ varies from 2 to 8. From the results

thus obtained, as depicted in Figures 3a-3c, which included five creeping wave modes, it can be seen that an order-of-magnitude reduction in the surface impedance produces no reduction in the back response of the element, provided the curved surface is still effectively rigid.

Again, for a nonuniform impedance surface with $Z_p = 20$ and Z_a varying from 0.1 to 10, we obtained the results depicted in Figures 4a-4c for the same variation in $k\rho_*^0$ from 2 to 8 via Equations (10), (21), and (24). Comparing these results with those of Figure 3, it should be noted that the diffraction patterns have lower main lobe to side lobe ratios than the latter as a consequence of the fact that they are all normalized with respect to the boresight response in a relatively rigid baffle (i.e., $Z_p = 20$). However, the dramatically reduced back response of Figure 4c is a direct consequence of the almost acoustically soft curved surface.

Finally, although it can be seen from Equations (16) and (17) that the attenuation coefficients remain constant for fixed values of $k\rho_*^0$, Equations (20) - (22) show that the receiver element directivity patterns will change via the diffraction coefficients and differential geometry of the surface as the dimensions of the ellipsoid vary.

Conclusions

We have reviewed the basic steps required to determine the role of diffraction on the back response of transducer array elements in uniform and nonuniform impedance baffles via the Geometrical Theory of Diffraction. In particular, we have considered the case of an ellipsoidally capped cylindrical baffle, neglecting the role of the transition zone between the insonified region of the array and the deep shadow zone, which has yet to be deduced analytically for an arbitrary impedance surface - a task

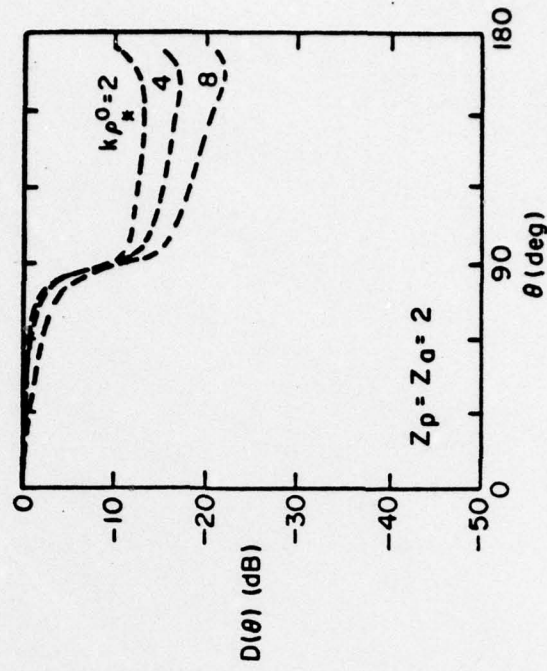


Fig. 3b Directional Response of a centrally located element in a uniform impedance baffle

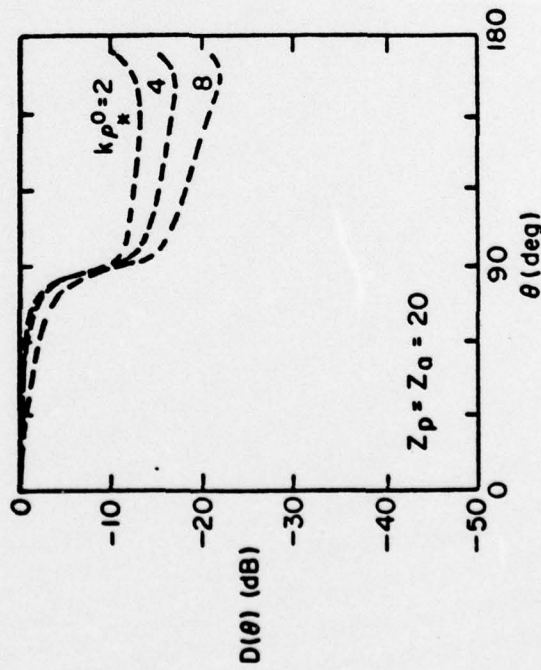


Fig. 3a Directional Response of a centrally located element in a uniform impedance baffle

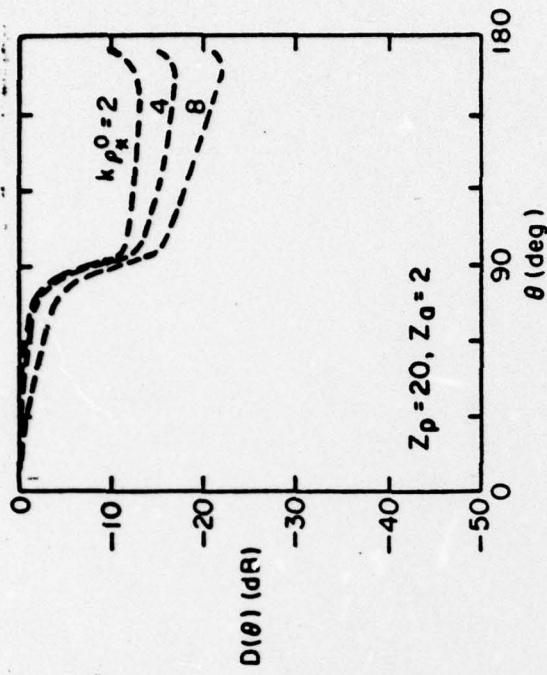


Fig. 4a

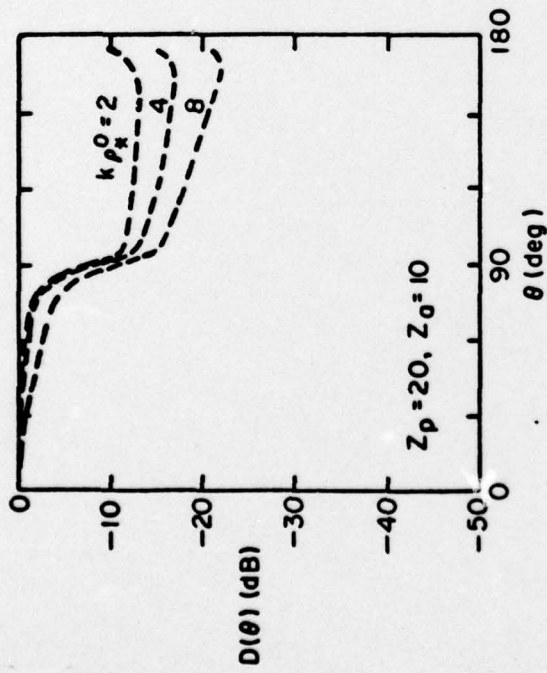


Fig. 4b

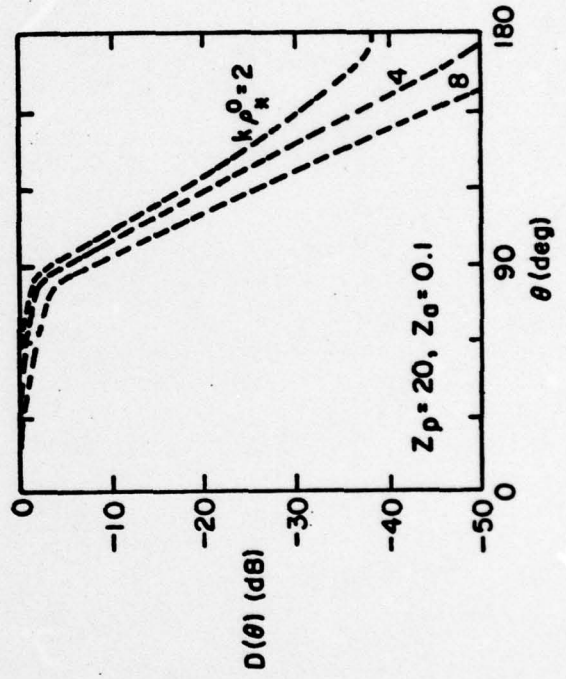


Fig. 4c

considerably beyond the scope of this preliminary investigation. We have also neglected to account for rapid changes in the radius-of-curvature on the diffraction and attenuation coefficients via 'correction factors' such as those derived by Voltmer⁹ for infinitely hard and infinitely soft surfaces. As in the case of the transition zone function, such correction factors have yet to be derived analytically for an arbitrary impedance surface. Other implicit limitations of the investigation also mitigated by its scope include the assumptions that the surface of the insonified body is locally reactive and impenetrable, i.e., the effect of flexural waves and internal sound waves on the array element response function is neglected. Nevertheless, despite these limitations, we believe that the approach taken in this paper is capable of providing a reasonable approximation of an array element response function on a nonuniform impedance, variable-radius-of-curvature surface provided $kp_*^0 \geq 2$.

APPENDIX A

In order to familiarize the reader with the derivation of 'diffraction' and 'attenuation' coefficients for the problem of the elliptically capped cylinder considered in this paper, we now review the underlying canonical problem of plane wave diffraction by an infinite circular cylinder of arbitrary impedance z_a . Locating an x, y coordinate system at the center of the cylinder, a plane wave incident field propagating along the x axis can be expressed in terms of the polar coordinates (r, θ)

$$\begin{aligned}
 p_i &= \exp(-ikx) \\
 &= \exp(-ikr \cos \phi) \\
 &= \sum_{m=-\infty}^{\infty} i^{-m} J_m(kr) \exp(im\phi) , \quad (A1)
 \end{aligned}$$

where the time dependence implicit in $\exp(j\omega t)$ is included post factum, and p_i is considered to be normalized with respect to its initial value. Since the scattered field p_s is composed of only outward going waves it can be expressed as a superposition of cylindrical waves weighted by the undetermined coefficients a_m as,

$$p_s = \sum_{m=-\infty}^{\infty} i^{-m} a_m H_m^{(2)}(kr) \exp(im\phi) . \quad (A2)$$

Combining the incident and scattered fields, Equations (A1) and (A2) respectively, the total acoustic field p becomes,

$$p = \sum_{m=-\infty}^{\infty} i^{-m} \{J_m(kr) + a_m H_m^{(2)}(kr)\} \exp(im\phi) \quad (A3)$$

In this instance, the boundary condition at the surface of the cylinder obtained from the linear constitutive equation (i.e., $p = z_a v$) assumes the form,

$$p + \frac{z_a}{ik} \frac{\partial p}{\partial r} \Big|_{r=a} = 0, \quad z_a = z_a / \rho_o c_o \quad (A4)$$

Hence,

$$a_m = - \left\{ \frac{iJ_m(\chi) + z_a J_m'(\chi)}{iH_m^{(2)}(\chi) + z_a H_m^{(2)'}(\chi)} \right\}_{\chi=ka} \quad (A5)$$

Substituting Equation (A5) in Equation (A3) and applying Watson's transformation (A1) the field p can be re-expressed via the identity

$$J_\nu(\chi) = \frac{1}{2} \{H_\nu^{(1)}(\chi) + H_\nu^{(2)}(\chi)\} \text{ as,}$$

$$p = \frac{1}{2\pi i} \int_{-\infty-i\epsilon}^{\infty-i\epsilon} \frac{\pi i e^{-i\nu\pi/2}}{1 - e^{-i2\nu\pi}} \left[H^{(1)}(kr) - \left\{ \frac{iH_\nu^{(1)}(\chi) + z_a H_\nu^{(1)'}(\chi)}{iH_\nu^{(2)}(\chi) + z_a H_\nu^{(2)'}(\chi)} \right\}_{\chi=ka} H_\nu^{(2)}(kr) \right] \times \{(-1)^{-\nu} e^{i\nu\phi} + (-1)^\nu e^{-i\nu\phi}\} d\nu \quad (A6)$$

Since the Hankel function of the first kind is analytic in the complex v -plane for large positive values of kr , it contributes nothing to the integral. However, the second term in the integrand has simple poles where $iH_\nu^{(2)}(\chi) + z_a H_\nu^{(2)'}(\chi) \Big|_{\chi=ka} = 0$. Denoting the roots of this equation by v_n , the residues of the integrand can be evaluated by expanding the denominator in a Taylor series about v_n such that

$$\begin{aligned}
 iH_{\nu}^{(2)}(x) + z_a H_{\nu}^{(2)'}(x) \Big|_{x=ka} &= iH_{\nu_n}^{(2)}(x) + z_a H_{\nu_n}^{(2)'}(x) \Big|_{x=ka} \\
 &+ (\nu - \nu_n) \frac{\partial}{\partial \nu} \{iH_{\nu}^{(2)}(x) + z_a H_{\nu}^{(2)'}(x)\} + \dots \\
 &= (\nu - \nu_n) \frac{\partial}{\partial \nu} \{iH_{\nu}^{(2)}(x) + z_a H_{\nu}^{(2)'}(x)\} \Big|_{\substack{x=ka \\ \nu=\nu_n}} \quad (A7)
 \end{aligned}$$

For $ka > 1$ since all values of ν_n have large negative imaginary components, $1 - e^{-12\nu_n\pi} \simeq 1$. Making this approximation, and utilizing the Wronskian relationship $H_{\nu_n}^{(1)}(ka) H_{\nu_n}^{(2)'}(ka) - H_{\nu_n}^{(1)'}(ka) H_{\nu_n}^{(2)}(ka) = 4/i\pi ka$, Equation (A6) can be reexpressed for $ka > 1$ as

$$P_d \simeq \frac{4}{ka} \sum_{n=1}^{\infty} H_{\nu_n}^{(2)}(kr) \left\{ \frac{e^{-i\nu_n(\pi/2 - \phi)} + e^{-i\nu_n(\pi/2 + \phi)}}{H_{\nu_n}^{(2)'}(ka) \left[\frac{\partial}{\partial \nu} H_{\nu}^{(2)}(ka) \right]_{\nu=\nu_n} - H_{\nu_n}^{(2)}(ka) \left[\frac{\partial}{\partial \nu} H_{\nu}^{(2)'}(ka) \right]_{\nu=\nu_n}} \right\} \quad (A8)$$

This solution can be further simplified by redefining the Hankel functions and their derivatives in terms of Airy functions as follows:

$$\frac{\partial}{\partial \nu} H_{\nu}^{(2)}(ka) \Big|_{\nu=\nu_n} = -H_{\nu_n}^{(2)'}(ka) = 2(2/ka)^{2/3} A_1'(-q_n) e^{-1\pi/3} \quad (A9a)$$

$$\frac{\partial}{\partial \nu} H_{\nu}^{(2)'}(ka) \Big|_{\nu=\nu_n} \simeq \frac{4}{ka} A_1''(-q_n) = -\frac{4\beta_n}{ka} A_1(-q_n) \quad (A9b)$$

$$\text{with } H_{\nu_n}^{(2)}(ka) \simeq 2(2/ka)^{1/3} A_1(-q_n) e^{1\pi/3} \quad (A9c)$$

$$\text{and } H_{\nu_n}^{(2)'}(ka) \simeq -2(2/ka)^{2/3} A_1'(-q_n) e^{-1\pi/3} \quad (A9d)$$

$$\text{where } A_1(-x) = \frac{1}{\pi} \int_0^{\infty} \cos(t^{2/3} - xt) dt, \text{ for } x \text{ real.} \quad (A10)$$

Substituting Equations (A9a) - (A9d) in Equation (A8) thus gives

$$P_d \approx -\frac{1}{2}(ka/2)^{1/3} e^{i2\pi/3} \sum_{n=1}^{\infty} \left\{ \frac{H_n^{(2)}(kr)}{A_1'^2(-q_n) + \beta_n A_1^2(-q_n)} \right\} \{ e^{-i\nu_n(\pi/2 - \phi)} + e^{-i\nu_n(\pi/2 + \phi)} \}$$

$$\approx \frac{e^{-ikr}}{\sqrt{r}} \left\{ \frac{\pi^{-1/2} 2^{-5/6} a^{1/3} e^{-i\pi/12}}{k^{1/6}} \right\} \sum_{n=1}^{\infty} \left\{ \frac{e^{-i\nu_n(\pi/2 - \phi)} + e^{-i\nu_n(\pi/2 + \phi)}}{A_1'^2(-q_n) + \beta_n A_1^2(-q_n)} \right\} \quad (\text{A11a})$$

$$= \frac{e^{-ikr}}{\sqrt{r}} \sum_{n=1}^{\infty} D_n^2 \{ e^{-i\nu_n(\pi/2 - \phi)} + e^{-i\nu_n(\pi/2 + \phi)} \} \quad (\text{A11b})$$

where the 'diffraction coefficients' D_n are defined as

$$D_n^2 = \frac{\pi^{-1/2} 2^{-5/6} k^{-1/6} a^{1/3} e^{-i\pi/12}}{A_1'^2(-q_n) + q_n A_1^2(-q_n)} \quad (\text{A12})$$

In addition,

$$\nu_n = ka - i\alpha_n a, \quad (\text{A13})$$

where the 'attenuation coefficients' are defined as

$$\alpha_n = \frac{q_n}{a} (ka/2)^{1/3} e^{i\pi/6} \quad (\text{A14})$$

Again, from Equations (A9c) and (A9d), since $iH_n^{(2)}(ka) + Z_a H_n^{(2)'}(ka) = 0$, it follows that

$$z_a = -1 \frac{H_n^{(2)}(ka)}{H_n^{(2)'}(ka)} \quad (\text{A15a})$$

$$= - \frac{e^{i\pi/6}}{(2/ka)^{1/3}} \frac{A_1(-q_n)}{A_1'(-q_n)} \quad (\text{A15b})$$

Alternatively,

$$\frac{A_1'(-q_n)}{A_1(-q_n)} = e^{i5\pi/6} (ka/2)^{1/3} z_a^{-1} \quad (\text{A16})$$

Now Equations (A12) and (A14) have exactly the same form as the respective diffraction and attenuation coefficients summarized by Pathak and Kouyoumjian.⁶ On the other hand, Levy and Keller⁵ employed a slightly different definition of the Airy function than that of Equation (A10), i.e.,

$$A_{LK}(-\chi_{LK}) = \int_0^{\infty} \cos(t^3 - \chi_{LK}t) dt, \quad \text{for } \chi_{LK} \text{ real} \quad (\text{A17})$$

Relating the terms in Equations (A10) and (A17) it follows that

$$A_{LK}(-\chi_{LK}) = \frac{\pi}{3^{1/3}} A_1(-\chi_{LK}/3^{1/3}) \quad (\text{A18})$$

$$A_{LK}'(-\chi_{LK}) = - \frac{\pi}{3^{2/3}} A_1'(-\chi_{LK}/3^{1/3}), \quad (\text{A19})$$

the roots q_n^{LK} of $A_{LK}(-q_n^{LK}) = 0$ being related to the roots β_n of $A_1(-\beta_n) = 0$ as

$$q_n^{LK} = 3^{1/3} q_n \quad (\text{A20})$$

Levy and Keller's² diffraction coefficients can thus be expressed as

$$D_n^{LK^2} = \frac{\pi^{3/2} 2^{-1/2} 6^{-1/3} k^{-1/6} a^{1/3} e^{-i\pi/12}}{3A_{LK}^{\prime 2}(-q_n^{LK}) + q_n^{LK} A_{LK}^2(-q_n^{LK})} \quad (A21)$$

and their attenuation coefficients as

$$\alpha_n^{LK} = \frac{q_n^{LK}}{a} (ka/6)^{1/3} e^{i\pi/6} , \quad (A22)$$

the impedance relationship being

$$\frac{A_{LK}^{\prime}(-q_n^{LK})}{A_{LK}(-q_n^{LK})} = e^{i5\pi/6} (ka/6)^{1/3} Z_a^{-1} . \quad (A23)$$

These diffraction and attenuation coefficients can then be used locally on a variable radius-of-curvature surface.

APPENDIX B

In order to obtain the roots of Equation (A23) we instead employ the more fundamental relationship Equation (A15a) from which it was derived, i.e.,

$$\frac{H^{(2)'}(ka)}{H^{(2)}(ka)} = iZ_a^{-1} ; \quad v_n = ka + (ka)^{1/3} \tau_n, \quad (B1)$$

where by comparison with Equations (A13), (A14), and (A20), as deduced by Keller,¹

$$q_n^{LK} = 6^{1/3} \tau_n e^{i\pi/3} \quad (B2)$$

Following Keller,¹ it can also be shown that for $ka \gg 1$

$$H_{v_n}^{(2)}(ka) \approx \frac{2^{5/4} e^{i\pi/4}}{\pi^{1/2} (ka)^{1/3} \tau_n^{1/4}} \cos\left\{\frac{\pi}{4} - \frac{1}{3}(2\tau_n)^{3/2}\right\} \quad (B3)$$

$$\text{and } \left. \frac{\partial H_{v_n}^{(2)}(\chi)}{\partial \chi} \right|_{\substack{v=v_n \\ \chi=ka}} \approx \frac{-2^{5/4} e^{i\pi/4}}{\pi^{1/2} (ka)^{1/3} \tau_n^{1/4}} (2\tau_n)^{1/2} \left\{ \sin \frac{\pi}{4} - \frac{1}{3}(2\tau_n)^{3/2} \right\}. \quad (B4)$$

Substituting Equations (B3) and (B4) in Equation (B1) thus gives Keller's¹ 'tangent approximation' for large ka ,

$$\begin{aligned} (2\tau_n)^{1/2} \tan\left\{\frac{\pi}{4} - \frac{1}{3}(2\tau_n)^{3/2}\right\} &= -(ka)^{1/3} Z_a^{-1} \\ \text{or } (2\tau_n)^{1/2} \tan\left\{\frac{1}{3}(2\tau_n)^{3/2} - \frac{\pi}{4}\right\} &= (ka)^{1/3} Z_a^{-1}. \end{aligned} \quad (B5)$$

This equation can then be solved numerically for τ_n as shown by Bremmer.^{B1}

For the asymptotic limit of an acoustically rigid surface (i.e., $Z_a = \infty$), Equation (B5) becomes

$$\sin\left[\frac{1}{3}(2\tau_n)^{3/2} - \frac{\pi}{4}\right] = 0 .$$

Hence,
$$\frac{1}{3}(2\tau_n)^{3/2} - \frac{\pi}{4} = n\pi$$

giving
$$\tau_n = \frac{1}{2}\{3\pi(n + \frac{1}{4})\}^{2/3} e^{-i\pi/3} , \quad n = 0, 1, 2, \dots \quad (B6)$$

Thus,
$$q_n^{LK} = \frac{6^{1/3}}{2} \{3\pi(n + \frac{1}{4})\}^{2/3} \quad \text{from Equation (B2) for } Z_a = \infty .$$

Alternatively, for the asymptotic limit of an acoustically soft surface (i.e., $Z_a = 0$), Equation (B5) becomes

$$\cos\left[\frac{1}{3}(2\tau_n)^{3/2} - \frac{\pi}{4}\right] = 0 .$$

Hence,
$$\frac{1}{3}(2\tau_n)^{3/2} - \frac{\pi}{4} = (n + \frac{1}{2}) \pi$$

giving
$$\tau_n = \frac{1}{2}\{3\pi(n + \frac{3}{4})\}^{2/3} e^{-i\pi/3} , \quad n = 0, 1, 2, \dots \quad (B7)$$

Thus,
$$q_n^{LK} = \frac{6^{1/3}}{2} \{3\pi(n + \frac{3}{4})\}^{2/3} \quad \text{from Equation (B2) for } Z_a = 0 .$$

It should be noted that the values of τ_0 and τ_1 appearing in Table 1b are exact estimates obtained by Bremmer^{B1} from the Airy function Equation (A23). Those obtained from Equations (B6) and (B7) are approximate to a few significant figures.

APPENDIX C

For the case of an edge element, or an element located in close proximity to an edge, the singularity in Equation (24) which occurs as the angle subtended by the element at the center of the coordinate system θ_0 approaches $\sin^{-1}(h_b/r_0)$ can be removed if each term in the creeping wave series is multiplied by Levy and Keller's⁵ correction factors R_n ,

$$\text{where } R_n = \frac{e^{ikR}}{\sqrt{h_b}} (2\pi k h_b)^{1/2} h_b \left(1 - \frac{r_0}{h_b} \sin\theta\right) I(k\rho_*, q_n^{LK}) \quad (C1)$$

$$\text{where } I(k\rho_*, q_n^{LK}) = \{e^{-i\pi/12} (k\rho_*/2)^{-2/3} A'_{LK}(-q_n^{LK}) [1 - (k\rho_*/2)^{-2/3} e^{i2\pi/3}] \\ + e^{i\pi/12} (k\rho_*/2)^{-1/3} A_{LK}(-q_n^{LK}) [1 + (k\rho_*/2)^{-2/3} e^{i2\pi/3}]\} \quad (C2)$$

$$\text{with } \rho_* = (a^2/b) (1 - \kappa^2 \sin^2 \psi)^{3/2} \quad (C3)$$

REFERENCES

1. J. B. Keller, "Diffraction by a Convex Cylinder," URSI Michigan Symposium on Electromagnetic Wave Propagation, Ann Arbor Michigan, June 1955.
2. J. B. Keller, "Geometrical Theory of Diffraction," J. Opt. Soc. Amer. 52, No. 2, 116-130 (1962).
3. W. Franz, "Über die Greenschen Funktionen des Zylinders und der Kugel," Z. Naturforsch. 9a, 705-716 (1954).
4. F. G. Leppington, "Creeping Waves in the Shadow of an Elliptic Cylinder," J. Inst. Maths. Applics. 3, 388-402 (1967).
5. B. R. Levy and J. B. Keller, "Diffraction by a Smooth Object," Comm. Pure and Appl. Math. 12, 159-209 (1959).
6. P. H. Pathak and R. G. Kouyoumjian, "An Analysis of the Radiation from Apertures in Curved Surfaces by the Geometrical Theory of Diffraction," Proc. I.E.E.E. 62, 1438-1447 (1974).
7. S. I. Hayek and A. D. Stuart, "Influence of an Elastic Plate Surface Impedance on Backscattered Sound," ARL Tech. Memorandum #74-255 (1974) (AD 001334).
8. D. A. Sachs, Unpublished Memorandum (1972).
9. D. R. Voltmer, "Diffraction by Doubly Curved Convex Surfaces," Ph.D. Dissertation, Ohio State University, Columbus, Ohio (1970).
- A1. G. N. Watson, "The Diffraction of Electrical Waves by the Earth," Proc. Roy. Soc. (London) A95, 83-99 (1918).
- B1. H. Bremmer, "Terrestrial Radio Waves," (Elsevier Inc., New York, 1949) p. 39, Eq. (14a).

DISTRIBUTION LIST -- TM 77-314

NAVSEA, Dr. E. G. Liszka, SEA-03421, Copy No. 1
NAVSEA, library, SEA-09G32, Copies No. 2 and 3
NSWC, Mr. C. B. Leslie, WU-21, Copy No. 4
NUSC, Mr. F. L. White, SB 332, Copy No. 5
NOSC, Mr. J. R. Campbell, Code 614, Copy No. 6
APL/UW, Mr. G. R. Sinfield, Copy No. 7
ARL/PSU, Dr. C. L. Ackerman, Copy No. 8
DDC, Copies 9 thru 20
Ohio State University, Electroscience Laboratory, Columbus, OH, 43212
Dr. Nar Wang, Copy No. 21
Admiralty Underwater Weapons Establishment, Portland, Dorset, England,
Mr. P. Madden, via British Navy Staff, Washington, DC, Copy No. 22
B. F. Goodrich Company, Research and Development Center, 9921 Brecksville Road,
Brecksville, OH 44141, Mr. S. J. Caprette, Copy No. 23